Tubular Aggregates of Cyclic Oligothiophenes. A Theoretical Study

Paola Flores, Patricia Guadarrama, Estrella Ramos, and Serguei Fomine*

Instituto de Investigaciones en Materiales, Universidad Nacional Autónoma de México, Apartado Postal 70-360, CU, Coyoacán, México DF 04510, México

Received: November 6, 2007; In Final Form: January 24, 2008

The geometries of neutral, mono-, and dioxidized tubular aggregates of cyclo[8]thiophenes containing up to 5 repeating units were fully optimized at the MPWB1K/3-21G* level of theory. Calculated interplane distances between macrocycles were found to be close to 3.1 Å for neutral and charged aggregates. The binding energies between macrocycles in neutral intermediates were in the range of 40−45 kcal/mol, increasing for monocations and dropping strongly for dicationic species due to electrostatic repulsion between polarons. It was established that there exists a noticeable interaction between π-orbitals of individual macrocycles in tubular aggregates as follows from decreasing of the band gap with a number of repeating units in aggregates and the polaron delocalization toward tube axes in oxidized species. A polaron pair is the most stable dicationic state for all studied molecules according to the calculations. A singlet polaron pair is more stable than a triplet one. The energy difference between singlet and triplet states is growing smaller with the size of the system, becoming zero for the pentamer corresponding to a completely dissociated bipolaron.

Introduction

Creation of hollow tubular structures by noncovalent self-assembly of appropriately crafted organic molecules has been the subject of considerable research in recent years.[1] Several computational studies employing DFT have focused on elucidating the electronic properties of cyclic-D,L-octapeptide nanotubes. The results suggest that intersubunit hydrogen bonding may delocalize electrons and holes toward the tube axis, so that band conduction might occur through the inter-ring hydrogen bonds.[2] More recently, the role of intra- and inter-ring hydrogen bonds in determining the electronic structure of peptide nanotubes has been examined, and it was found that the electronic band-edge states are strongly dependent on the inter-ring hydrogen bonds.[3] DFT calculations have predicted a large gap in the low-energy electronic excitation spectrum, with both extended and localized states near the gap.[4]

Well-defined π-conjugated macrocycles are of interest as modular building blocks for the assembly of new materials[5] and supramolecular architectures. Due to their toroidal structure, they could represent molecular circuits which would additionally include sites for recognition and selective complexation. In this respect, it is necessary to mention recently synthesized, fully conjugated macrocyclic structures: cyclo(oligothiophene−diacetylenes) and cyclo[*n*]thiophenes capable of self-assembling to hexagonal nanoarrays and forming unique 1:1 π-donor−π-acceptor complexes with C60, representing excellent candidates for self tubular assembling.[6]

Polythiophenes and their corresponding finite model oligothiophenes belong to the most investigated conjugated systems due to their chemical stability in different redox states, their excellent electronic and transport properties in the solid state, the various possibilities of functionalization, as well as their potential application in molecular electronic devices.[7] Although, to the best of our knowledge, there were no reports on tubular self-assembling of cyclo[*n*]thiophenes, other π-conjugated macrocycles and polymers such as oligophenylacetylenes[8] and oligoterphenylobiphenylenes[9] are known to form tubular structures bonded by interactions between aromatic units. Notably, the tubules in aqueous solution can solubilize single-walled carbon nanotubes through $\pi-\pi$ interactions.[9] Although physical properties of cyclo[*n*]thiophenes were investigated both experimentally and theoretically,[10] neither experimental nor theoretical studies were reported dealing with tubular self-assembling of cyclo[*n*]thiophenes.

The aim of this study is to explore stability and electronic properties of neutral and ionized tubular aggregates of cyclo-[8]thiophene, the smallest synthesized cyclic oligothiophene, to predict important features of those nanoaggregates using quantum chemistry tools.

Computational Details

The modeling of complexes bonded by mostly dispersion interactions is a challenging task requiring methods taking into account dynamic correlation. The Hartree−Fock (HF) theory does not take into account dispersion interactions, while the most popular functionals perform very poorly because they fail to reproduce correctly the dispersion terms.[11] On the other hand, even the least computationally demanding post-HF method, MP2 theory, is prohibitive for the smallest aggregate; cyclo[8]-thiophene dimer renders the modeling of cyclo[8]thiophene aggregates a challenging task.

Different new hybrid meta functionals[12] designed for modeling of noncovalent interactions were tested against the MP2 model for the cyclo[4]thiophene dimer. The results of these tests show that the meta hybrid functional MPWB1K[12] reproduces the geometry of cyclo[4]thiophene dimer optimized at the MP2 level within 0.01−0.02 Å, even in the case of the most challenging interplane distances while other popular functionals like B3LYP and PBE0 gave interplane distances by 0.2−0.3 Å longer, evidencing poor performance for noncovalent interactions. MPWB1K is based on the modifed Perdew−Wang 1991 exchange functional[13] and Becke's 1995 meta correlation

10.1021/jp710654k CCC: $40.75
Published on Web 03/18/2008

functional,[14] where meta means that it depends on kinetic energy density as well as the density and the gradient of density. The MPWB1K functional is available in Gaussian 03 through a combination of keywords; mpwb95 and iop(3/76 = 0560004400). In a very recent paper,[15] it has been shown that the MPWB1K functional performed well for stacking interactions and H_2, Ne, and N_2 encapsulation into C60.[16] Therefore, the MPWB1K functional in combination with the 3-21G* basis set was used for all geometry optimizations. The comparison of calculated binding energies for the cyclo[4]thiophene dimer obtained at MPWB1K/3-21G* and LMP2/cc-PVDZ//MP2/3-21G* levels (3.18 and 3.50 kcal/mol, respectively) proves this model to be able to reproduce reasonably well MP2 energy results for weakly interacting systems as well.

Restricted HF formalism was used for neutral systems while unrestricted HF was applied to monoionized and diionized systems, respectively. Cyclo[8]thiophene and tubular aggregates of cyclo[8]thiophene containing from 2 to 5 monomer units were fully optimized without any symmetry restrictions. All calculations were carried out with Gaussian 03 suit of programs.[17] Time-dependent (TD) DFT calculations were carried out using MPWB1K/3-21G* optimized geometry at the B3LYP/6-31G* level. This level of theory gives band gaps of 4.26, 3.36, 2.48, and 1.89 eV for the thiophene dimer, trimer, hexamer, and polythiophene (oligomer containing 40 repeating units), close to the corresponding experimental data of 4.12,[18] 3.2,[19] 3.0 ± 0.6,[20] and 2.0 eV,[21] respectively.

Tubular aggregates of cyclo[8]thiophene and linear oligomers are denoted as ***n*C8** and **L*n*** where ***n*** is the number of cyclo-[8]thiophene units in the aggregate or linear oligomer, respectively. Mono and diionized systems are referred to as + and **+2 (+2-T** and **+2-S)**, where **S** and **T** correspond to the singlet and triplet states, respectively.

To ensure that the tubular structure is the global minimum on the potential energy surface, in the case of dimers two more possible structures were fully optimized—T-shaped and parallel-displaced, similar to those for benzene. The calculations revealed that the tubular structure of **2C8** is far more stable than T-shaped (by 37.1 kcal/ mol) and parallel-displaced (by 21.2 kcal/mol) structures.

Results and Discussion

Neutral Aggregates. Figure 1 and Table 1 show optimized geometries and interplane distances in oligocyclo[8]thiophene nanoaggregates. As seen, the interplane distances are not changed significantly with the number of oligocyclo[8]thiophene units being close to 3.1 Å. In the cases of **4C8** and **5C8**, the interplane distances between inner macrocycles are more uniform compared to outer macrocycles, suggesting different binding between oligocyclo[8]thiophenes fragments in different positions. Table 2 shows calculated binding energies in tubular nanoaggregates of oligocyclo[8]thiophene. As seen from Table 2, the binding energies between macrocycles are very significant, ranging from 38.7 to 44.8 kcal/mol depending on the macrocycle position in the aggregate. The highest binding energy of 44.8 kcal/ mol was found for **2C8**, while the weakest binding was detected for the central macrocycle in **5C8**. As seen, the binding between macrocycles is strong enough to form stable tubular aggregates. Although the interplane distances in neutral aggregates are not uniform, there is a correlation between the binding energies and shortest interplane distances between macrocycles. Thus, as seen from Tables 1 and 2 in the case of stronger bonded lateral macrocycles in **3C8**, **4C8**, and **5C8**, the shortest observed interplane distances are smaller for stronger bonded outer rings. The band gap estimation using the TD-B3LYP/6-31G*//MPWB1K/3-21G* level of theory (Table 3) shows that there is a noticeable interaction between π-orbitals of macrocycles forming the aggregate. It is seen that there is a trend of narrowing the band gap with the number of macrocycles, similar to that observed in conjugated polymers with the number of repeating units. Thus, the band gap decreases from 2.60 eV for **C8** to 2.49 eV for **5C8**. Even for **5C8** the band gap is larger compared to that of polythiophene. Figure 2 shows the most important molecular orbitals (MOs) involved in the S0→S1 transition. In all cases except **3C8** the most important contribution is from HOMO−LUMO excitation, while for **3C8** HOMO−LUMO+1 excitation dominates the transition. As seen from Figure 2, MOs are delocalized over the entire tubular aggregate showing that S0→S1 excitation is global in character, similar to excitation in a conjugated polymer.

Unlike linear oligomers where thiophene units have anti conformations leading to a planar structure of the polythiophene chain, the most stable conformation of thiophene rings in **C8** is *sin*, resulting in the nonplanar geometry of **C8** cycles due to steric hindrances caused by sulfur atoms (Figure 1). It is known that nonplanarity of a polymer chain leads to the band gap increase in conjugated polymers. Therefore, systematically larger band gaps of tubular aggregates compared to linear analogues are due to the nonplanar geometry of **C8** units.

Monocations. The first step in the oxidative doping of a conjugated polymer is the formation of a cation radical (polaron). Cationic species are responsible for the hole transport phenomenon by a hopping-type mechanism between adjacent molecules or chains accompanied by geometric relaxation.[22]

Table 3 shows vertical (IP_v) and adiabatic (IP_a) ionization potentials for studied aggregates. The difference between vertical and adiabatic IP represents the relaxation energy (λ) that is a measure of the mobility of a polaron in a conjugated system. Generally, the relaxation energies decrease with oligomer chain length as a result of greater positive charge delocalization in a longer oligomer.[23] IP_v reflects the conjugation in a neutral molecule and the ability of the electronic system to stabilize positive charge. As noted in Table 3, both vertical and adiabatic IPs decrease with the number of thiophene macrocycles similar to that in linear conjugated systems reflecting participation of all macrocycles in the stabilization of positive charge. Both vertical and adiabatic IPs decrease more rapidly for tubular aggregates of cyclooligothiophenes with the number of thiophene units than for linear oligothiophenes, evidencing better ability of the positive charge stabilization in large tubular structures. Thus, **5C8** has even slightly lower IP_a compared to **L40**. This is due to much greater deformability of tubular aggregates leading to an increase of relaxation energies. The relaxation energies are linearly related to the square root of the chain length of the linear oligomers.[23] The relaxation energies are larger for cyclic oligothiophenes[24] compared to linear oligomers owing to greater geometry change in cyclic cation radicals on ionization. In the case of tubular aggregates, the relaxation energies are also higher compared to those of linear analogues. As shown in Table 3, the relaxation energy drops from **C8** to **3C8** and then slightly increases to **5C8**. As mentioned above, the relaxation energy for linear oligomers decreases with polaron delocalization. The delocalization of a polaron depends not only on the oligomer length but also on its deformability. High deformability of a conjugated system increases the relaxation energy. The deformability of tubular aggregates can be estimated by comparing energies obtained from the full and partial optimization runs. The most remote atoms in fully optimized structures of tubular

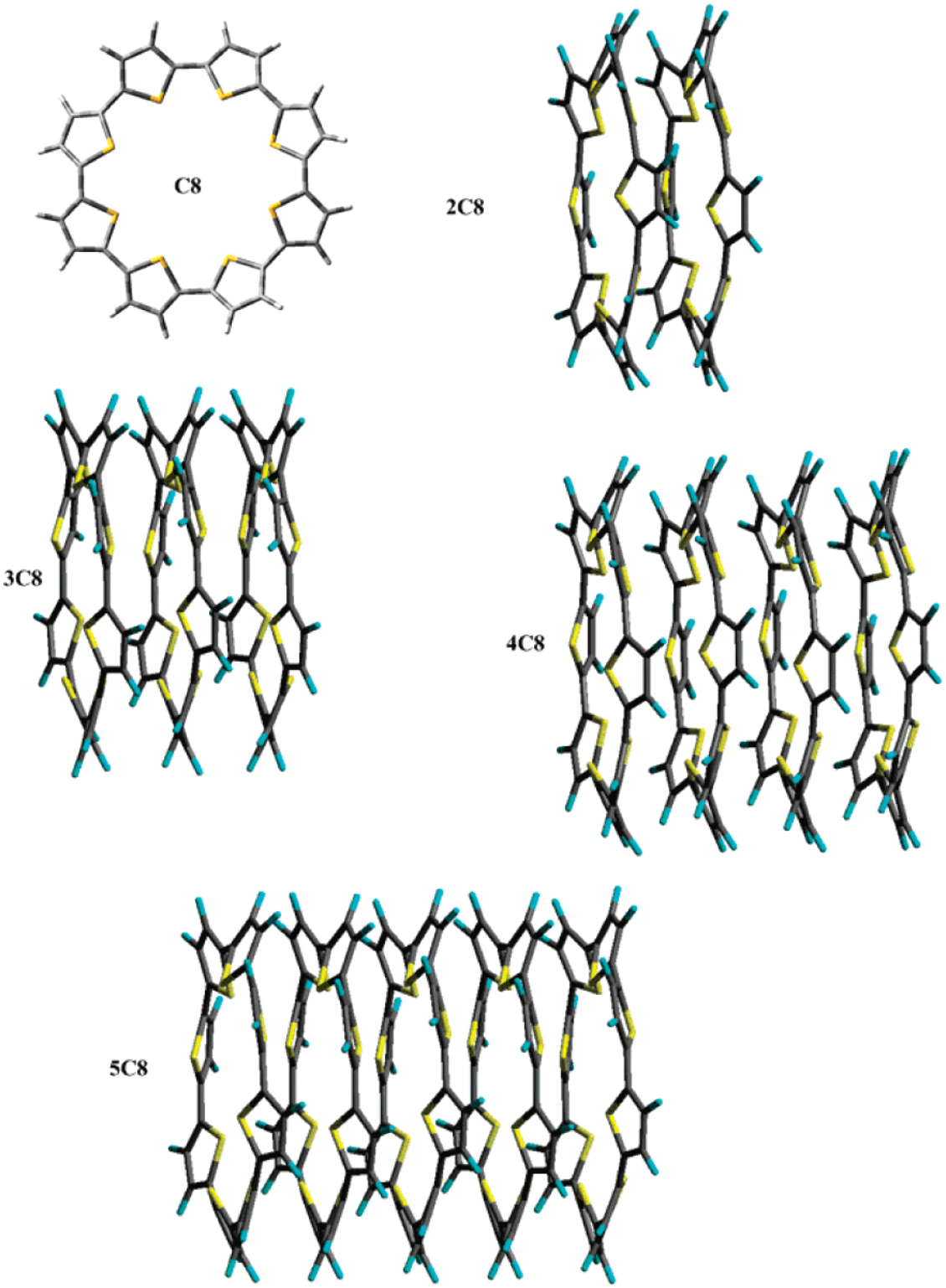

Figure 1. MPWB1K/3-21G* optimized geometries of neutral tubular aggregates.

aggregates were frozen and the distances between them were increased by 1 Å compared to totally relaxed geometry, and the geometry optimization was repeated using new settings. The energy difference (ΔE_d) between totally and partially optimized structures is the measure of their deformability. Thus, ΔE_d found for **C8**, **2C8**, **3C8**, **4C8**, and **5C8** are 5.8, 6.3, 7.1, 4.4, and 4.3 kcal/mol, respectively. As seen, the deformability decreases from **C8** to **3C8** and then increases to **5C8** in line with calculated relaxation energies for monocations. Therefore, the unusual behavior of the relaxation energy is directly related to the deformability of tubular aggregates.

Since a polaron represents a cation radical, the unpaired electron density distribution can be used as a measure of polaron delocalization (Figure 3). As seen, the polaron is distributed uniformly across the macrocycles in **C8**+ and **2C8**+, while in larger aggregates the polaron is localized mostly at inner macrocycles. Thus, in **4C8**+ and **5C8**+, polarons are localized mostly at two and three inner macrocycles, respectively. The

TABLE 1: Calculated Interplane Distances between Thiophene Rings in Oligocyclo[8]thiophene Tubular Aggregates (Å)

aggregate	**1−2**[a]	**2−3**[a]	**3−4**[a]	**4−5**[a]
2C8	3.07			
3C8	3.06−3.12	3.07−3.13		
4C8	3.05−3.13	3.11−3.12	3.05−3.13	
5C8	3.05−3.15	3.09−3.11	3.08−3.11	3.06-3.16
2C8+	3.07−3.08			
3C8+	3.08−3.11	3.07−3.11		
4C8+	3.05−3.12	3.09−3.11	3.05−3.13	
5C8+	3.06−3.12	3.09−3.11	3.09−3.11	3.06−3.12
2C8+2-S	3.09−3.11			
3C8+2-S	3.06−3.12	3.06−3.12		
4C8+2-S	3.08−3.12	3.11−3.13	3.08−3.12	
5C8+2-S	3.07−3.12	3.10−3.12	3.10−3.13	3.07−3.12
2C8+2-T	3.06−3.09			
3C8+2-T	3.07−3.14	3.08−3.14		
4C8+2-T	3.08−3.12	3.12−3.13	3.08−3.13	
5C8+2-T	3.07−3.12	3.10−3.12	3.10−3.12	3.07−3.12

[a] The index numbers of macrocycles.

TABLE 2: Calculated Binding Energies between Oligocyclo[8]thiophene Macrocycles in Tubular Aggregates (kcal/mol)

aggregate	**1−2**[a]	**2−3**[a]	**3−4**[a]	**4−5**[a]
2C8	44.8	-	-	-
3C8	42.9	42.9	-	-
4C8	41.3	39.4	41.3	-
5C8	42.1	38.7	38.7	42.1
2C8+	50.9			
3C8+	47.8	47.8		
4C8+	44.9	48.1	44.9	
5C8+	44.8	45.0	45.0	44.8
2C8+2-S	9.65			
3C8+2-S	15.5	15.5		
4C8+2-S	20.3	17.2	20.3	
5C8+2-S	26.1	20.1	20.1	26.1
2C8+2-T	5.15			
3C8+2-T	13.11	13.11		
4C8+2-T	20.0	16.9	16.9	20.0
5C8+2-T	26.1	20.1	20.1	26.1

[a] The index numbers of a macrocycles.

TABLE 3: Vertical (IP_v) and Adiabatic (IP_a) Ionization Potentials, Corresponding Relaxation Energies (λ_1, λ_2) (eV), and the Band Gaps (E_g) of Tubular Aggregates and Linear Oligothiophenes

molecule	IP_{v1}[a]	IP_{a1}[a]	λ_1[c]	IP_{v2}[b]	IP_{a2}[b]	λ_2[d]	E_g
C8	6.58	6.33	0.25	8.82	8.60	0.22	2,60
2C8	6.21	6.06	0.15	8.26	8.12	0.14	2,53
3C8	5.97	5.84	0.13	7.84	7.73	0.11	2,54
4C8	5.82	5.68	0.14	7.55	7.40	0.15	2,52
5C8	5.74	5.57	0.17	7.41	7.14	0.27	2,49
L8	6.19	6.02	0.17	8.20	8.06	0.14	2.28
L16	5.93	5.85	0.08	6.91	6.75	0.16	1.98
L24	5.83	5.78	0.05	6.49	6.39	0.10	1.92
L32	5.76	5.71	0.05	6.30	6.24	0.06	1.89
L40	5.73	5.71	0.02	6.30	6.10	0.20	1.88

[a] First ionization potential. [b] Second ionization potential. [c] Relaxation energy is the energy difference between the first vertical and adiabatic ionization potentials. [d] Relaxation energy is the energy difference between the second vertical and adiabatic ionization potentials

obtained results are in line with calculations on cyclic-D,L-octapeptide nanotubes.[2] It was demonstrated that inter-ring interaction may delocalize electrons and holes toward the tube axis.

Table 3 shows the binding energies in cation radicals. As can be noted, the binding energies in cation radicals are always larger compared to those in neutral aggregates. Therefore, monooxidation should favor the self-assembling of macrocycles. This phenomenon is due to additional polarization stabilization of charged macrocycles by neighbor neutral rings. A similar effect was observed for cation radicals of catenanes containing cyclic oligothiophenes.[24] On the other hand, the interplane distances between macrocycles are close to those found for neutral aggregates, as evidenced from the Table 1.

Dications. It has been shown earlier[10h] that a singlet restricted solution is unstable with respect to an unrestricted one for linear, cyclic dicationic states of oligothiophenes and dicationic states of oligothiophene catenanes and knots. A restricted solution corresponds to a bipolaron defect, while an unrestricted one corresponds to a polaron pair. When a linear oligomer contains less that 6−8 repeating units, the unrestricted solution is converged to a restricted one, reflecting the impossibility of the bipolaron dissociation. Our calculations also confirmed this finding for tubular aggregates of cyclic oligothiophenes.

Table 4 shows the relative energies of dications of tubular aggregates and linear oligothiophenes for different spin states. As can be seen, the unrestricted solution is always more stable compared to the restricted one for singlet states, for both linear oligomers and tubular aggregates. Moreover, the energies of open-shell singlets are similar or lower compared to triplet states. The difference reaches 7.07 kcal/mol for **C8+2**, and the relative stability of triplet states increases with the number of thiophene units in linear oligothiophenes or tubular aggregates. In the case of linear oligothiophenes, open-shell singlet and triplet states become practically degenerated for **L16**, corresponding to a completely dissociated polaron pair. For tubular aggregates of cyclic oligothiophenes, a complete dissociation of a polaron pair has occurred already for **5C8+2** where triplet and open-shell singlet states become degenerated by energy. It has been shown earlier[24b] that in the case of excessive confinement, the doubly charged defects are generally more localized in the triplet state due to additional restriction imposed by Pauli repulsion leading to the energy increase of such states.

Similar to cation radicals, the unpaired electron density distribution can be used as a measure of polaron delocalization in dications.

Figure 4 shows the spin density distribution in open-shell singlet dicationic states of **C8** and the corresponding tubular aggregates. As seen, even in the **C8+2-S** molecule there is a visible separation of two polarons reflected in a difference of 0.55 kcal/mol between restricted and unrestricted solutions. A similar situation holds for the dimer and trimer where two polarons are being dissociated not between but rather within each macrocycle. For the tetramer and pentamer (**4C8+2-S** and **5C8+2-S**), the situation is different; in these cases each polaron is located at different macrocycles to minimize the electrostatic repulsion. As seen from Figure 4, in **5C8+2-S** the polarons are completely separated. The separation of polarons in dications can also be monitored by the comparison of the energy difference between open-shell singlet and triplet states of dications. As seen from Table 4, this difference decreases with the number of macrocycles in tubular aggregates, becoming zero for **5C8+2** where polarons are completely separated.

Second ionization potentials for dications follow the trend found for the first ionization potentials dropping with the number of macrocycles in tubular aggregates. In this case, however, the second IP of a tubular aggregate is always higher than that of the linear analogue. Similar to the first relaxation energy (λ_1), the second relaxation energy (λ_2) for tubular aggregates is larger

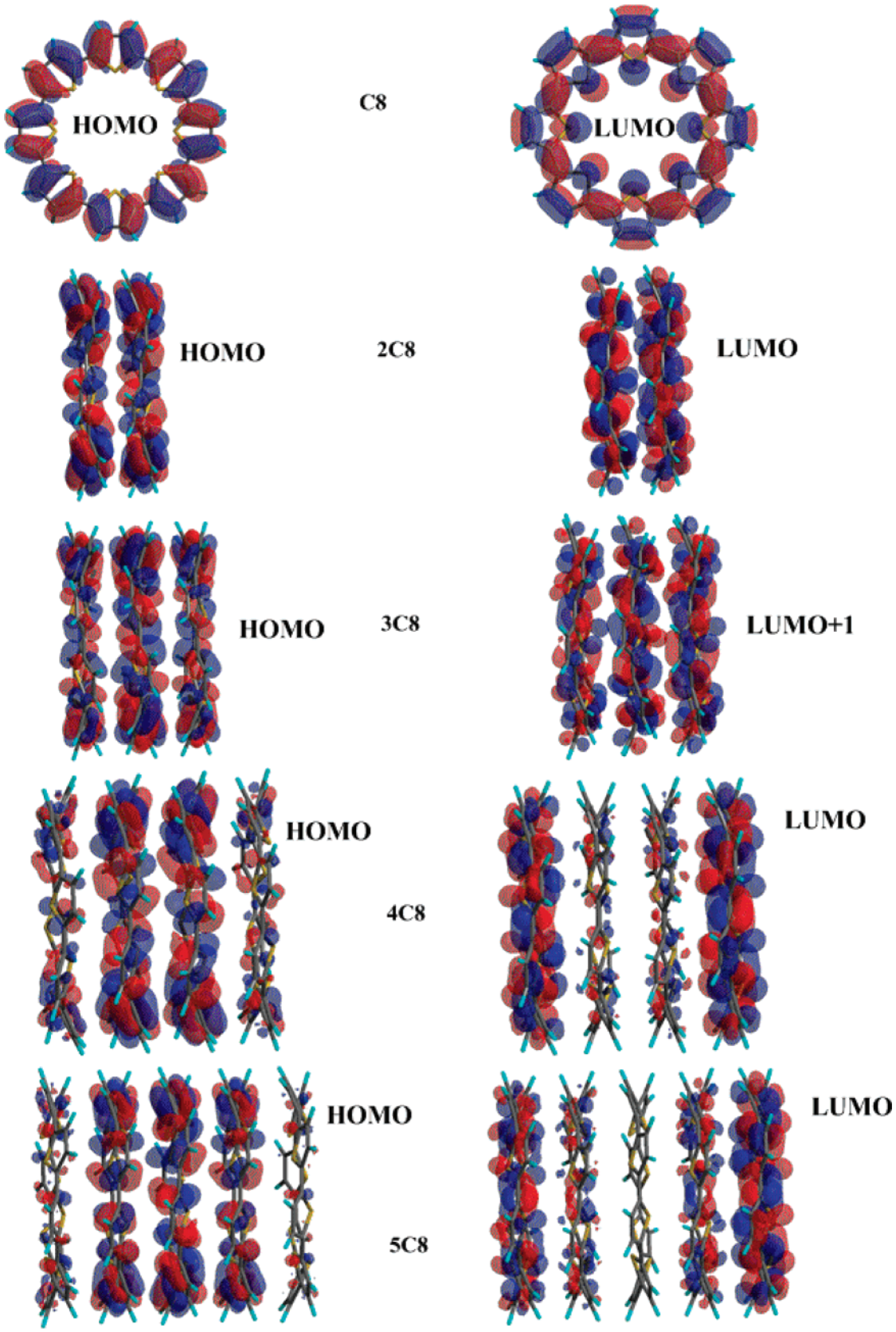

Figure 2. Molecular orbitals of neutral aggregates involved in the S0→S1 transition calculated at B3LYP/6-31G*//MPWB1K/3-21G* level of theory.

compared to that of linear oligomers with the same number of thiophene units due to higher deformability of tubular aggregates.

Unlike the first ionization, the second ionization weakens the inter-ring interactions (Table 2). As seen, the calculated binding energy in **2C8**+**2-S** is only 9.65 kcal/mol, that is one-fifth of that for the dimer monocation **2C8**+. For larger aggregates, however, the binding energy increases; even for the pentamer dication (**5C8**+**2-S**) the binding energy between macrocycles is less than half of that for the monocation. Such a strong drop

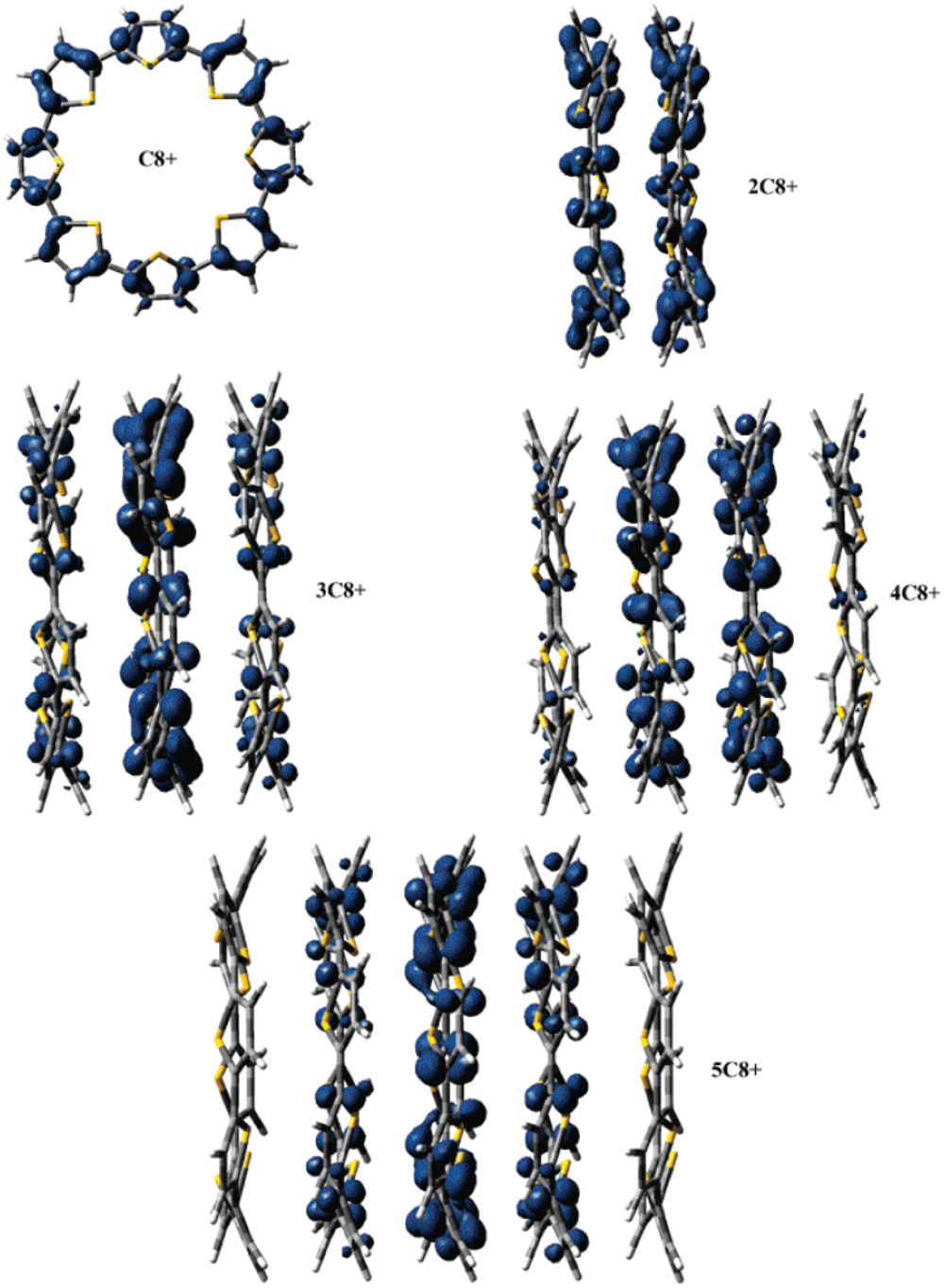

Figure 3. MPWB1K/3-21G* optimized geometries and unpaired spin density distribution in cation radicals of tubular aggregates.

of binding energy between macrocycles in dications is an indication of electrostatic repulsion between polarons. Polaron dissociation in large tubular aggregates decreases this repulsion, favoring binding between macrocycles. As seen from the calculations, the first ionization favors the stabilization of tubular aggregates, while the formation of dications leads to their strong destabilization and could even result in their dissociation, especially in the case of the dimer **2C8**+**2-S**. A very weak bonding in the dimeric dication is reflected in increasing the interplane distances for this aggregate from 3.07 to 3.08 Å for neutral and monoionized dimers to 3.09−3.11 Å for the dication **2C8**+**2-S**. In larger dications, this increase is not as pronounced due to delocalization of positive charge; however, interplane distances in all dications are constantly larger compared to neutral and monocationic systems reflecting weaker binding in

TABLE 4: Energy Difference between the Triplet and Open-Shell Singlet (ΔE_1), and between Closed-Shell Singlet and Open-shell Singlet (ΔE_2) Dications (kcal/mol), and Expectation Value of the S^2 Operator for Triplet $\langle S_t^2 \rangle$ and Open-Shell Singlets $\langle S_{oss}^2 \rangle$

molecule	ΔE_1 (kcal/mol)	ΔE_2 (kcal/mol)	$\langle S_{oss}^2 \rangle$	$\langle S_t^2 \rangle$
C8+**2**	−7,07	−0,55	0.52	2.08
2C8+**2**	−4,50	−0,61	0.50	2.03
3C8+**2**	−2,07	−0.31	0.43	2.03
4C8+**2**	−0,21	−1,57	0.94	2.02
5C8+**2**	−0,00	−3,73	1.00	2.02
L8+**2**	−1.98	−6.24	1.05	2.08
L16+**2**	−0.09	−13.91	1.13	2.12
L24+**2**	0.00	−11.52	1.10	2.10
L32+**2**	0.00	−9.09	1.06	2.06
L40+**2**	0.00	−7.38	1.03	2.03

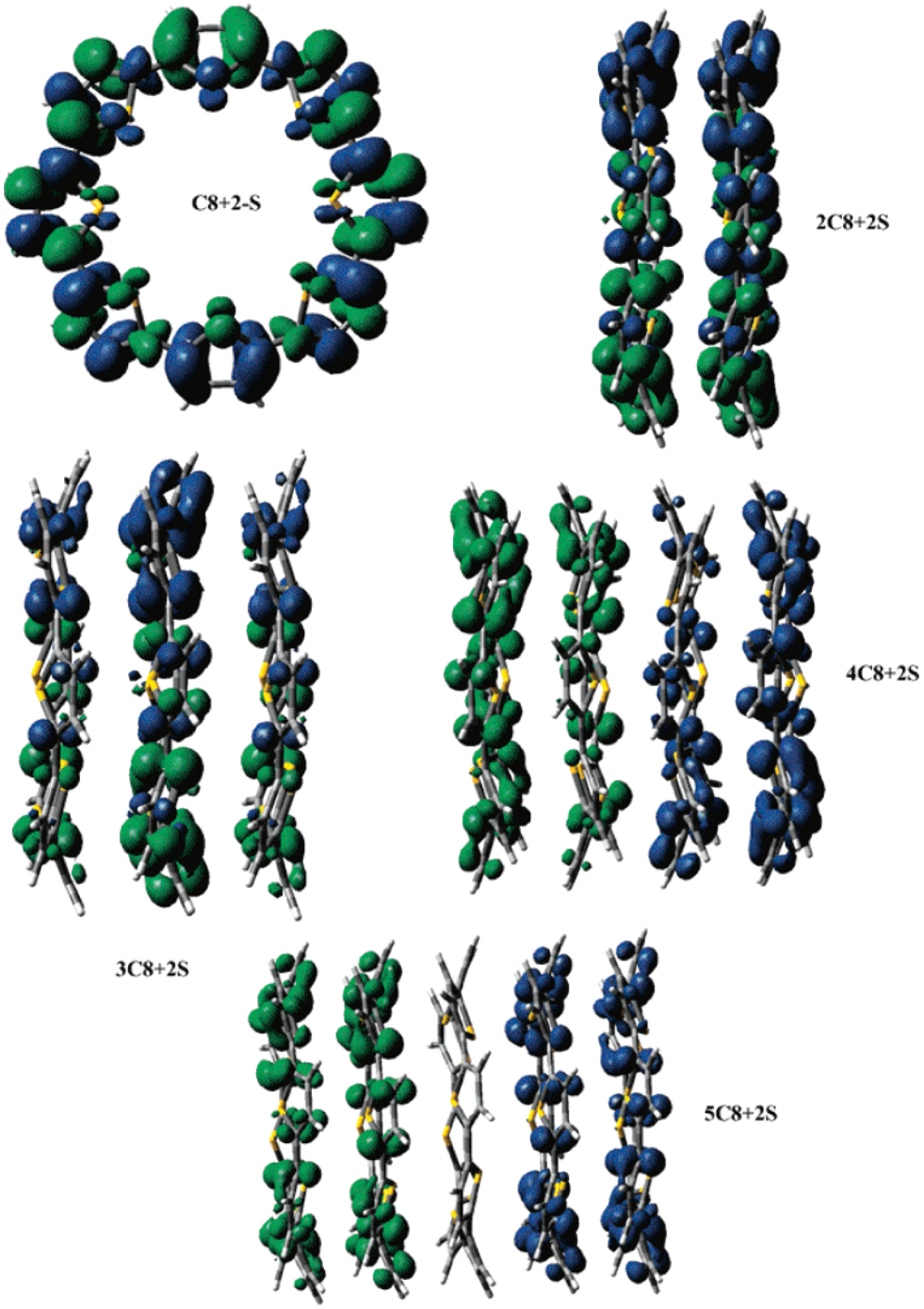

Figure 4. MPWB1K/3-21G* optimized geometries and unpaired spin density distribution in singlet dications of tubular aggregates. Different colors correspond to α and β electrons, respectively.

the former. The Cartesian coordinates of all optimized structures can be found in Supporting Information.

Conclusion

The calculations demonstrated that high binding energies between macrocycles in neutral aggregates (40−45 kcal/mol) render them as promising candidates for self-assembling. Neutral tubular aggregates easily lose an electron converting into cation radicals. The IP_a for **4C8** and **5C8** are even lower than for the corresponding linear polythiophenes. The binding in cations between macrocycles is higher compared to neutral aggregates favoring self-assembling on oxidation. The oxidation of neutral aggregates leads to polaron formation. The polaron is delocalized toward the tube axes, while most of it is located at the central macrocycles. The relaxation energies in tubular aggregates are higher compared to linear polythiophenes with the same number of repeating units due to their higher deformability.

A polaron pair, not a bipolaron, is the most stable dicationic state for all studied aggregates. A singlet polaron pair is more stable than a triplet one. This difference is growing smaller with the size of the system corresponding to a completely dissociated bipolaron, becoming zero for the pentamer. The binding energy between macrocycles decreases strongly in dications due to the electrostatic repulsion between polarons. This effect is especially important for small aggregates that could lead to their dissociation into smaller monocationic aggregates.

Acknowledgment. This research was carried out with the support of Grant 49290 from CONACyT.

Supporting Information Available: Optimized Cartesian coordinates. This material is available free of charge via the Internet at http://pubs.acs.org.

References and Notes

(1) (a) Lehn, J.-M. *Supramolecular Chemistry*; VCH: Weinheim, Germany, 1995. (b) Gattuso, G.; Menzer, S.; Nepogodiev, S. A.; Stoddart, J. F.; Williams, D. J. *Angew. Chem., Int. Ed. Engl.* **1997**, *36*, 1451. (c) Nelson, J. C.; Saven, J. G.; Moore, J. S.; Wolynes, P. G. *Science* **1997**, *227*, 1793. (d) Cram, D. J. *Nature* **1992**, *356*, 29. (e) Abrahams, B. F.; Hoskins, B. F.; Michael, D. M.; Robson, R. *Nature* **1994**, *369*, 727. (f) Venkataraman, D.; Lee, S.; Zhang, J. S.; Moore, J. S. *Nature* **1994**, *371*, 591.

(2) Fukasaku, K.; Takeda, K.; Shiraishi, K. *J. Phys. Soc. Jpn.* **1997**, *66*, 3387.

(3) Okamoto, H.; Kasahara, M.; Takeda, K.; Shiraishi, K. *Pept. Sci.* **1999**, *36*, 67.

(4) Carloni, P.; Andreoni, W.; Parrinello, M. *Phys. Rev. Lett.* **1997**, *79*, 761.

(5) Moore, J. S.; Zhang, J. *Angew. Chem., Int. Ed. Engl.* **1992**, *31*, 922.

(6) (a) Fuhrmann, G.; Debaerdemaeker, T.; Bäuerle, P. *Chem. Commun.* **2003**, 948. (b) Krömer, J.; Ríos-Carreras, I.; Fuhrmann, G.; Musch, C.; Wunderlin, M.; Dabaerdemaeker, T.; Mena-Osteritz, E.; Bäuerle, P. *Angew. Chem., Int. Ed.* **2000**, *39*, 3481. (c) Mena-Osteritz, E.; Bäuerle, P. *Adv. Mater.* **2006**, *18*, 447.

(7) (a) *Handbook of Oligo and Polythiophenes*; Fichou, D., Ed.; Wiley-VCH: Weinheim, Germany, 1999. (b) Horowitz, G.; Peng, X.; Fichou, D.; Garnier, F. *J. Appl. Phys.* **1990**, *67*, 528. (c) Paloheimo, J.; Kuivalainen, P.; Stubb, H.; Vuorimaa, E.; Yli-Lahti, P. *Appl. Phys. Lett.* **1990**, *56*, 1157. (d) Perepichka, I. F.; Perepichka, D. F.; Meng, H.; Wudl, F. *Adv. Mater.* **2005**, *17*, 2281−2305. (e) Geiger, F.; Stoldt, M.; Schweizer, H. (f) Bäuerle, P.; Umbach, E. *Adv. Mater.* **1993**, *5*, 922. (f) Brabec, C. J.; Sariciftci, N. S.; Hummelen, J. C. *Adv. Funct. Mater.* **2001**, *11*, 15. (g) Hoppe, H.; Sariciftci, N. S. *J. Mater. Res.* **2004**, *19*, 1924.

(8) (a) Prince, R. B.; Barnes, S. A.; Moore, J. S. *J. Am. Chem. Soc.* **2000**, *122*, 2758. (b) Zhang, J.; Moore, J. S. *J. Am. Chem. Soc.* **1994**, *116*, 2655.

(9) Ryu, J.-H.; Oh, N.-K.; Lee, M. *Chem. Commun.* **2005**, 1770.

(10) (a) Fuhrmann, G.; Debaerdemaeker, T.; Bäuerle, P. *Chem. Commun.* **2003**, 948. (b) Krömer, J.; Ríos-Carreras, I.; Fuhrmann, G.; Musch, C.; Wunderlin, M.; Dabaerdemaeker, T.; Mena-Osteritz, E.; Bäuerle, P. *Angew. Chem., Int. Ed.* **2000**, *39*, 3481. (c) Bednarz, M.; Rwineker, P.; Mena-Osteritz, E.; Baüerle, P. *J. Lumin.* **2004**, *110*, 225. (d) Casado, J.; Hernández, V.; Ponce Ortíz, R.; Ruíz Delgado, M. C.; López, Navarrete, J. T.; Fuhrmann, G.; Bäuerle, P. *J. Raman Spectrosc.* **2004**, *35*, 592. (e) Mena-Osteritz, E.; Bäuerle, P. *Adv. Mater.* **2001**, *13*, 243. (f) Mena-Osteritz, E. *Adv. Mater.* **2002**, *14*, 609. (g) Mena-Osteritz, E.; Bäuerle, P. *Adv. Mater.* **2006**, *18*, 447. (h) Sanjio, S. Z.; Bendikov, M. *J. Org. Chem.* **2006**, *71*, 2972.

(11) Chaasinski, G.; Szczniak, M. M. *Chem. Rev.* **2000**, *100*, 4227.

(12) Yan, Zhao, Y.; Truhlar, D. G. *J. Phys. Chem. A* **2004**, *108*, 6908.

(13) Perdew, J. P.; Wang, Y. *Phys. Rev. B* **1992**, *45*, 13244.

(14) Becke, A. D. *J. Chem. Phys.* **1996**, *104*, 1040.

(15) Dkhissi, A.; Blossey, R. *Chem. Phys. Lett.* **2007**, *439*, 35.

(16) Slanina, Z.; Pulay, P.; Nagase, S. *J. Chem. Theory Comput.* **2006**, *2* (3), 782.

(17) Frisch, M. J.; Trucks, G. W.; Schlegel, H. B.; Scuseria, G. E.; Robb, M. A.; Cheeseman, J. R.; Zakrzewski, V. G.; J. Montgomery, A.; Stratmann, R. E., Jr.; Burant, J. C.; Dapprich, S.; Millam, J. M.; Daniels, A. D.; Kudin, K. N.; Strain, M. C.; Farkas, O.; Tomasi, J.; Barone, V.; Cossi, M.; Cammi, R.; Mennucci, B.; Pomelli, C.; Adamo, C.; Clifford, S.; Ochterski, J.; Petersson, G. A.; Ayala, P. Y.; Cui, Q.; Morokuma, K.; Malick, D. K.; Rabuck, A. D.; Raghavachari, K.; Foresman, J. B.; Cioslowski, J.; Ortiz, J. V.; Baboul, A. G.; Stefanov, B. B.; Liu, G.; Liashenko, A.; Piskorz, P.; Komaromi, I.; Gomperts, R.; Martin, R. L.; Fox, D. J.; Keith, T.; Al-Laham, M. A.; Peng, C. Y.; Nanayakkara, A.; Challacombe, M.; Gill, P. M. W.; Johnson, B.; Chen, W.; Wong, M. W.; Andres, J. L.; Gonzalez, C.; Head-Gordon, M.; Replogle, E. S.; Pople, J. A. *Gaussian 03*; Gaussian, Inc.: Wallingford, CT, 2004.

(18) Brédas, J. L.; Silbey, R.; Boudreaux, D. S.; Chance, R. R. *J. Am. Chem. Soc.* **1983**, *105*, 6555.

(19) Choi, Y.; Tepavcevic, S.; Xu, Z.; Hanley, L. *Chem. Mater.* **2004**, *16*, 1924.

(20) Tepavcevic, S.; Wroble, A. T.; Bissen, M.; Wallace, D. J.; Choi, Y.; Hanley, L. *J. Phys. Chem. B* **2005**, *109*, 7134.

(21) Kobayashi, M.; Chen, J.; Chung, T.-C.; Moraes, F.; Heeger, A. J.; Wudl, F. *Synth. Met.* **1984**, *9*, 77.

(22) (a) Brédas, J. L.; Calbert, J. P.; da Silva, D. A.; Cornil, J. *Proc. Natl. Acad. Sci. U.S.A.* **2002**, *99*, 5804. (b) Cornil, J.; Beljonne, D.; Calbert, J. P.; Brédas, J. L. *Adv. Mater.* **2001**, *13*, 1053.

(23) Hutchison, G. R.; Ratner, M. A.; Marks, T. J. *J. Am. Chem. Soc.* **2005**, *127*, 2339.

(24) (a) Fomine, S.; Guadarrama, P. *J. Phys. Chem. A* **2006**, *110*, 10098. (b) Fomine, S.; Guadarrama, P.; Flores, P. *J. Phys. Chem. A* **2007**, *111*, 3124.